

Angular BN-Heteroacenes with *syn*-Structure-Induced Promising Properties as Host Materials of Blue Organic Light-Emitting Diodes

Wanzheng Zhang,[†] Fan Zhang,^{*,†} Ruizhi Tang,[†] Yubin Fu,[‡] Xinyang Wang,[†] Xiaodong Zhuang,[†] Gufeng He,^{*,§} and Xinliang Feng^{†,‡}

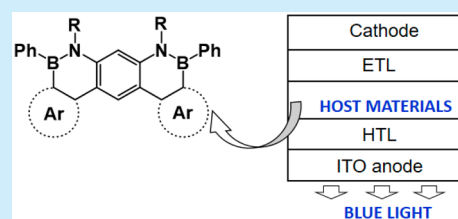
[†]School of Chemistry and Chemical Engineering, State Key Laboratory of Metal Matrix Composites, Shanghai Jiao Tong University, Shanghai 200240, P. R. China

[§]National Engineering Lab for TFT-LCD Materials and Technologies, Department of Electronic Engineering, Shanghai Jiao Tong University, Shanghai 200240, P. R. China

[‡]Center for Advancing Electronics Dresden (cfaed) and Department of Chemistry and Food Chemistry, Technische Universität Dresden, 01062 Dresden, Germany

Supporting Information

ABSTRACT: A series of novel angular BN-heteroacenes were successfully synthesized. Associated with the intrinsic *syn*-structures, they exhibit unique molecular alignments in a solid state and promising electronic properties, and are thus suitable as efficient nondoped emitters for the fabrication of blue organic light-emitting diodes with improved performance.



Numerous acenes have attracted considerable attention for their rich electronic properties applicable in various electronic devices such as organic field-effect transistors and organic light-emitting diodes (OLEDs).¹ In particular, the versatile chemical modification of these molecule types allows for the continuous improvement of their characteristics and processability.² The most common approach for improving the optoelectronic properties or self-assembly behavior of a heteroacene molecule is to attach it to the substituted groups in the molecular periphery and embed multiple heteroatoms such as N, S, Si, P, or B in the molecular main backbone.³ Some heteroacenes embedded with the isoelectronic B–N units of C=C units exhibit similar geometric structures but substantially different electronic behaviors relative to their all-carbon analogues, which have been studied as biomedical and organic electronic materials in recent years.⁴ We previously reported the first example of blue OLED devices based on BN-heteroacenes.^{4b} Subsequently, Nakamura et al. reported that BN-polycyclic aromatic hydrocarbons were formed by the replacement of the central C=C unit of boradibenzo[*g,p*]-chrysene with a B–N unit, which showed high singlet–triplet excitation energy. Phosphorescent OLEDs using these BN-molecules as host materials exhibited higher efficiencies and longer device lifetimes than did the representative host material 4,4'-bis(*N*-carbazolyl)-1,1'-biphenyl (CBP).^{4d} However, the lack of the species of BN-containing heteroacenes remains a major obstacle for deeper exploration of molecules such as luminescent components for the fabrication of high-quality blue OLED devices.

Altering molecular symmetry has become an efficient approach for tuning the electronic structure, self-organization

behavior, and environmental stability of heteroacene molecules.⁵ In previous reports, the *syn*-/*anti*-isomers of heteroacenes have mainly been studied in field-effect transistors, demonstrating that *anti*-isomers always exhibit a higher performance than do *syn*-isomers.⁶ Recently, Ma et al. found that heteroacenes with *syn*-structures indicated comparatively favorable properties for the fabrication of high-performance electroluminescent devices, likely associated with the different intermolecular orientation and dipole moments from their *anti*-isomers.⁷ Although the synthesis and structural characterization of some angular acenes/heteroacenes featuring *syn*-structures, such as dibenz[*a,j*]anthracene (I) and dithienyl[*a,j*]anthracene (II) (Figure 1), have been described previously,⁸ their

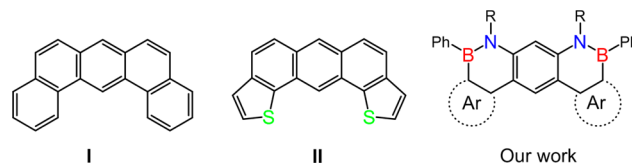


Figure 1. Typical structures of angular-fused aromatics.

properties and potential application have not yet been presented. From this viewpoint, there remains various possibilities for developing new angular *syn*-heteroacenes in synthesis, properties, and device fabrication.

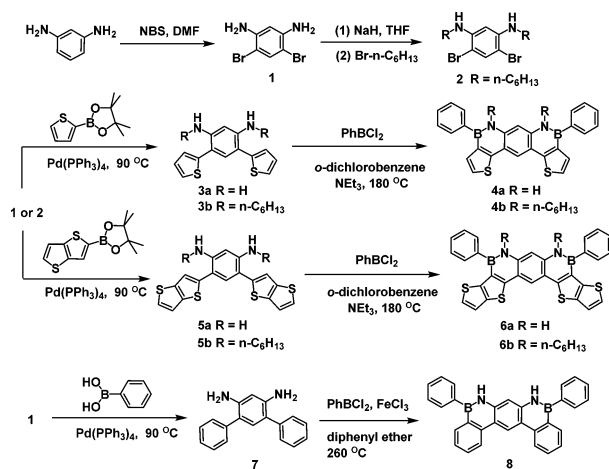
Herein, we report the concise synthesis of a series of novel angular *syn*-BN-heteroacenes through nitrogen-directed aro-

Received: June 8, 2016

matic borylation. Their geometric and electronic structures were investigated systematically through X-ray crystallography, optical spectroscopy, and cyclic voltammetry (CV). We also explored the possibility of using these BN-heteroacenes as dopant-free host active materials for blue OLED device fabrication.

The target angular BN-heteroacenes were synthesized as shown in Scheme 1. We first synthesized 1,3-dibromo-4,6-

Scheme 1. Synthetic Approach to the Target Angular BN-Heteroacenes



diaminobenzene (**1**) through the bromination of 1,3-phenylenediamine with 2 equiv of *N*-bromosuccinimide in *N,N*-dimethylformamide at 0 °C, which was further transformed to 1,3-dibromo-4,6-*N*⁴,*N*⁶-dihexyl benzene-diamine (**2**) in 50% yield by attaching a hexyl group on each nitrogen atom. The key intermediates 1,3-bis-heterocycle-substituted phenylenediamines (**3a**, **3b**, **5a**, **5b**, **7**) were then prepared through Suzuki coupling of **1** or **2** with the corresponding aryl boronic ester or boronic acid. Upon treatment with excess PhBCl₂ by using triethylamine as a base in *o*-dichlorobenzene under refluxing overnight, thienyl ring-fused angular BN-heteroacenes (**4a,b** and **6a,b**) were readily achieved with 2-fold electrophilic cyclization through nitrogen-directed borylation on the bilateral thiophene rings of **3a,b** and **5a,b** in high yields (>70%).

However, under similar reaction conditions, the intermediate **7** cannot be converted to the target compound **8**, probably because the electron-poor benzene ring is unfavorable for electrophilic attack. Under the excess PhBCl₂ and FeCl₃ in diphenyl ether, heating to 260 °C for 8 h readily converted diamino intermediates into BN-fused acenes. After purification through chromatography on silica gel, compound **8** was obtained as a pale yellow powder in a yield of 35%. This result might provide a simple and efficient pathway for the transformation of BN-embedded aromatics.

All new compounds were fully characterized through ¹H, ¹³C, and ¹¹B NMR spectroscopy and through high-resolution mass spectrometry. Typically, a broad peak appeared at approximately 4 ppm in the ¹H NMR spectra (CDCl₃), which was attributed to the protons of the amino groups of the intermediates **3a**, **5a**, and **7**. After the formation of the corresponding BN-heteroacenes **4a**, **6a**, and **8** by cyclization, no signal was observed in this region; instead, the chemical shifts for the protons in the nitrogen sites were located at approximately 9.5–10.6 ppm (SI, Figures S8, S18, and S26),

suggesting the aromatic characteristic of the BN-fused rings in these as-prepared molecules.^{4,9} ¹¹B NMR spectra of these target compounds displayed broad singlet peaks at approximately 35–38 ppm in CDCl₃, indicating the presence of three-coordinated boron atoms.^{4,9} These BN-embedded heteroacenes exhibited excellent thermal stability with a weight loss of 5% at approximately 380 °C on the basis of a thermogravimetric analysis (SI, Figures S29–33).

The molecular structures were further confirmed through X-ray crystallography (Figure 2). Yellow single crystals of **4b** and

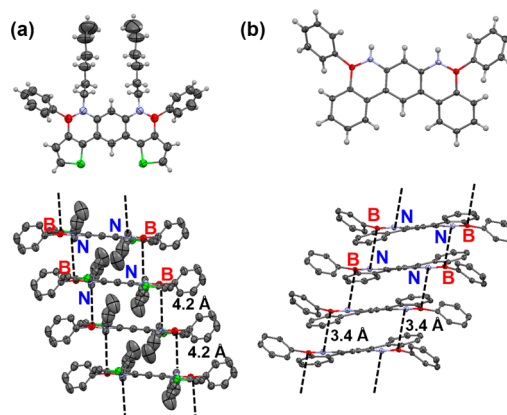


Figure 2. ORTEP drawing crystal structures (50% probability for thermal ellipsoid) and packing diagrams for **4b** (a) and **8** (b), respectively.

8 suitable for X-ray single-crystal analysis were obtained by slowly diffusing hexane into a dichloromethane solution at room temperature. The BN bond lengths of **4b** and **8** were 1.428 and 1.408 Å, respectively, featuring double-bond character.⁴ The dihedral angles between the central benzene ring and BN-containing six-membered ring were 2.7° and 9.1° for **4b** and **8**, respectively, relative to their nearly planar and S-shape bending backbones. The substituted phenyl groups were strongly twisted and deviated from the mean planes of the main backbones by approximately 62.5° for **4b** and 47.1° for **8**, respectively. The crystals of **4b** exhibited a staggered packing pattern. In each of the π -stacked columns, the molecules were alternatively oriented to the reverse directions, adopting a face-to-face slipped stacking. A distance of 4.2 Å between B and N atoms in the neighboring molecules, nearly equal to the shortest distance between the layers, was observed, suggesting no apparent intermolecular π - π interaction. This *syn*-molecule showed a significantly different solid packing motif compared with its *anti*-structure isomer in our previous report.^{4b} The molecules of **8** adopted a herringbone packing arrangement, exhibiting a similar alignment in each π -stacked column in **4a**, but a markedly shorter BN distance of 3.4 Å between the neighboring layers, manifesting in the distinct B...N dipole interaction associated with their Lewis bases and acid characters. Clearly, embedding BN units not only led to a fused aromatic skeleton with π -extend system but also created a unique intermolecular B...N supermolecular linkage and was thus favorable for strengthening intermolecular interactions. Such efficient B...N interaction at a distance of less than 4.0 Å has rarely been observed in BN-embedded molecules.⁹ The unique solid state of this type of *syn*-BN-heteroacene might improve its electronic properties, performance, and applicability in device fabrication.¹⁰

The UV–vis absorption spectra of these *syn*-BN-heteroacenes were measured in CH₂Cl₂, displaying two sets of absorption peaks from 250 to 500 nm (Figure 3a, Table 1).

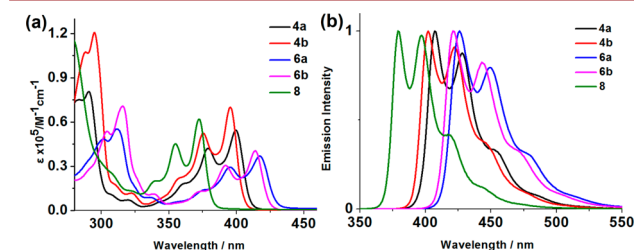


Figure 3. (a) UV–vis absorption spectra and (b) normalized fluorescence spectra at 10^{−5} M in CH₂Cl₂.

Table 1. Photophysical Data for the As-Prepared *syn*-BN-Heteroacenes

	UV–vis absorption		fluorescence		
	λ_{abs}^a (nm)	log ϵ	λ_{em} (nm)	Φ_{PL}^b	τ (ns)
4a	400	4.74	407	0.42/0.04	2.7
4b	396	4.85	402	0.40/0.11	2.5
6a	417	4.57	426	0.52/0.01	1.9
6b	414	4.61	421	0.48/0.11	3.1
8	372	4.79	379	0.17/0.06	2.7

^aIn CH₂Cl₂ (10^{−5} M), only the longest λ_{max} values were provided.

^bAbsolute values in CH₂Cl₂ (10^{−5} M) and in solid.

Compared with 4a and 4b, the main absorption bands of 6a and 6b with larger π -systems were red-shifted by approximately 18 nm. Compound 8 fused with phenyl groups at the terminal positions, demonstrating maximum absorption peaks at 372 nm with blue-shifts of 23 and 27 nm compared with 4a and 4b fused with thiophene terminal groups, respectively. This phenomenon was likely due to either the higher planarity of 4a or 4b, as shown by the aforementioned crystal analysis or their richer electron density contributed by thiophene moieties. The optical band gaps were calculated on the basis of the absorption edges to be in the order of 3.24 eV (8) > 3.05 eV (4b) > 3.02 eV (4a) > 2.92 eV (6b) > 2.89 eV (6a), which is consistent with their increased electron-donating and extended π -conjugated characteristics. Additionally, their main absorption bands in the thin films broadened and red-shifted relative to those in the solution, demonstrating their stronger intermolecular interactions while in the solid state (SI, Figures S35–39).

The fluorescence spectra of these *syn*-BN-heteroacenes exhibited blue luminescence with emission maxima from 379 to 426 nm (Figure 3b), blueshifted by approximately 10 nm relative to their position in the isomers of *anti*-BN-heteroacenes in our previous reports.^{4b} The relatively low Stokes shift values of 7–9 nm (Table 1) for these *syn*-BN-heteroacenes reveal less structural deformation upon excitation relative to that in the ground state. Notably, the fluorescence quantum yields of compounds 4a, 4b, 6a, and 6b (from 0.40 to 0.52) in solution are considerably higher than those of *anti*-BN-heteroacenes. A similar phenomenon was also observed in a recent report on pyrene-imidazole-based structural isomers.⁷ By contrast, a moderate luminescent quantum yield ($\Phi_{\text{PL}} = 0.17$) for compound 8 can probably be attributed to the strong intermolecular interaction observed in the crystallography analysis. The fluorescence quantum yields of compounds 4a,

6a, and 8 in solid state are much lower than those of 4b and 6b, probably attributable to the decreased intermolecular interactions in the latter case, associated with their long alkyl chains at nitrogen atoms. The fluorescence lifetimes of these molecules showed slight differences, indicating their similar excited states (Table 1).

The electrochemical behaviors of these *syn*-BN-heteroacenes were investigated through CV in CH₂Cl₂. The CV profiles exhibited irreversible oxidation processes under the measurement conditions (SI, Figure S34). The first oxidation potentials gradually increased in the order of 6a < 6b < 4b–8 < 4a. Accordingly, their highest occupied molecular orbital (HOMO) energy levels were evaluated from the onset of the first oxidation potentials in the order of 4a (−5.40 eV) < 4b–8 (−5.39 eV) < 6b (−5.34 eV) < 6a (−5.29 eV), demonstrating that a π -extended backbone raises the HOMO energy level for these types of BN-heteroacenes. Moreover, the lowest unoccupied molecular orbital (LUMO) energy levels were evaluated on the basis of the HOMO values and optical band gaps, with a sequence of 6b (−2.42 eV) < 6a (−2.40 eV) < 4a (−2.38 eV) < 4b (−2.34 eV) < 8 (−2.15 eV). Generally, minor modification on either the main backbone or molecular periphery can fine-tune the molecular electronic structures of as-prepared heteroacenes.

To gain insight into the electronic structures of these *syn*-BN-heteroacenes, theoretical calculations based on density functional theory (RB3LYP/6-31G(d) level) were performed (SI). For example, in each case for compounds 4a and 8, either the HOMO or LUMO was approximately distributed over the entire main backbone (Figures 4 and S52, SI). For compound

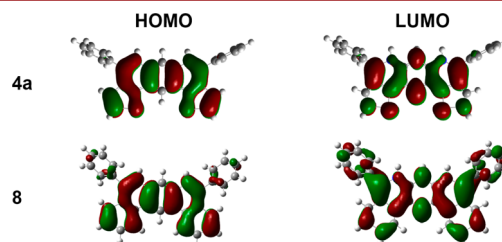


Figure 4. Calculated molecular orbitals of compounds 4a and 8.

8, these frontier orbitals were located at the two phenyl rings attached to the boron atoms, which lead to an enlarged electron delocalization over the whole molecular skeleton. The calculated LUMO and HOMO values are summarized in Table S1, demonstrating a tendency similar to that of the experimental results.

Developing excellent organic blue light-emitting materials for high-quality full-color displays and solid-state lighting applications remains a considerable challenge. The as-prepared *syn*-BN-heteroacenes exhibited promising optical properties, such as high luminescent quantum yield, which encouraged us to use them as nondoped emitters for fabricating blue OLED devices. A series of OLED devices were fabricated with the sandwich configuration of ITO/NPB (50 nm)/X = 4a (I), 4b (II), 6a (III), 6b (IV) (30 nm)/TPBI (30 nm)/LiF (1 nm)/Al (100 nm), where NPB, X, and Alq₃ were used as hole-transporting, light-emitting, and electron-transporting layers, respectively (SI). The initial performance of devices without optimization is summarized in Table 2. Among the devices, the electro-luminescence spectra of the 4b-based device (II) displayed an emission maximum at 426 nm, red-shifted by 24 nm relative to

Table 2. EL Device Performance^a

	V_{on} (V)	λ_{EL} (nm)	η_{c} (cd/A)	$\eta_{\text{c,max}}$ (cd/A)	η_{p} (lm/W)	η_{ext} (%)	CIE (x,y)
I	2.8	479	0.92	1.07	0.69	0.48	0.23, 0.32
II	3.0	426	0.58	0.85	0.34	0.63	0.20, 0.17
III	2.7	491	2.68	2.68	2.55	1.06	0.26, 0.44
IV	2.8	474	0.99	1.22	0.69	0.70	0.18, 0.25

^aAbbreviations: V_{on} , voltage required for 1 cd m⁻²; η_{c} , current efficiency measured at 100 cd m⁻²; η_{p} , power efficiency measured at 100 cd m⁻²; η_{ext} measured at 100 cd m⁻².

its photoluminescence data. Additionally, the electroluminescence emission maxima of the devices based on **4a** (I), **6a** (III), or **6b** (IV) exhibited larger redshifts (53–72 nm) compared with the corresponding photoluminescence data. These devices exhibited lower turn-on voltages, less than 3.0 V, compared with those of the *anti*-BN-heteroacene-based devices,^{4b} suggesting that the as-prepared *syn*-BN-heteroacenes could offer favorable carrier transport for OLED devices.¹¹ Device III had a starting voltage of 2.7 V, $\eta_{\text{c,max}}$ of 2.7, and external quantum efficiency (EQE) of 1.06%, ranking it the most effective of the heteroacene-based blue OLED devices.¹¹ These results strongly support the hypothesis that molecular symmetry enables efficient improvement of the fabrication and performance of OLED devices.

In summary, we successfully designed and synthesized a new family of angular BN-heteroacenes, featuring *syn*-structures that provide them with unique molecular arrangements in the solid state and significantly improved their photophysical properties in comparison with their *anti*-isomers. These *syn*-BN-heteroacenes were used as nondoped light-emitting host materials to fabricate blue OLED devices that demonstrated favorable performance including a low starting potential without optimization. Our group is continuing to modify these *syn*-BN-heteroacenes to improve their electronic properties to create high-performance blue OLED devices. Additionally, the potential utilization of changes in molecular symmetry to develop new types of promising organic materials is worthy of further investigation.

■ ASSOCIATED CONTENT

Supporting Information

The Supporting Information is available free of charge on the ACS Publications website at DOI: 10.1021/acs.orglett.6b01659.

Experimental details, NMR spectra, UV–vis spectra, fluorescence spectra, cyclic voltammetry, and single-crystal X-ray diffraction data (PDF)

Compound **4b** (CIF)

Compound **8** (CIF)

■ AUTHOR INFORMATION

Corresponding Authors

*E-mail: fan-zhang@sjtu.edu.cn.

*E-mail: gufenghe@sjtu.edu.cn.

Notes

The authors declare no competing financial interest.

■ ACKNOWLEDGMENTS

We are grateful for the financial supported from the National Basic Research Program of China (973 Program: 2013CBA01602, 2012CB933404), the Natural Science Foun-

dation of China (21574080), and the Shanghai Committee of Science and Technology (15JC1490500).

■ REFERENCES

- (1) (a) Anthony, J. E. *Angew. Chem., Int. Ed.* **2008**, *47*, 452. (b) Anthony, J. E. *Chem. Rev.* **2006**, *106*, 5028.
- (2) (a) Mei, J.; Diao, Y.; Appleton, A. L.; Fang, L.; Bao, Z. N. *J. Am. Chem. Soc.* **2013**, *135*, 6724. (b) Chaskar, A.; Chen, H. F.; Wong, K. T. *Adv. Mater.* **2011**, *23*, 3876.
- (3) (a) Jiang, W.; Li, Y.; Wang, Z. H. *Chem. Soc. Rev.* **2013**, *42*, 6113. (b) Fukazawa, A.; Yamaguchi, S. *Chem. - Asian J.* **2009**, *4*, 1386.
- (4) (a) Hatakeyama, T.; Hashimoto, S.; Seki, S.; Nakamura, M. *J. Am. Chem. Soc.* **2011**, *133*, 18614. (b) Wang, X. Y.; Zhang, F.; Liu, J.; Tang, R. Z.; Fu, Y. B.; Wu, D. Q.; Xu, Q.; Zhuang, X. D.; He, G. F.; Feng, X. L. *Org. Lett.* **2013**, *15*, 5714. (c) Wang, X. Y.; Zhuang, F. D.; Wang, R. B.; Wang, X. C.; Cao, X. Y.; Wang, J. Y.; Pei, J. *J. Am. Chem. Soc.* **2014**, *136*, 3764. (d) Hashimoto, S.; Ikuta, T.; Shiren, K.; Nakatsuka, S.; Ni, J.; Nakamura, M.; Hatakeyama, T. *Chem. Mater.* **2014**, *26*, 6265. (e) Wang, X. Y.; Zhuang, F. D.; Wang, X. C.; Cao, X. Y.; Wang, J. Y.; Pei, J. *Chem. Commun.* **2015**, *51*, 4368. (f) Li, G.; Xiong, W. W.; Gu, P. Y.; Cao, J.; Zhu, J.; Ganguly, R.; Li, Y. X.; Grimsdale, A. C.; Zhang, Q. C. *Org. Lett.* **2015**, *17*, 560.
- (5) (a) Xie, Z. Q.; Yang, B.; Li, F.; Cheng, G.; Liu, L. L.; Yang, G. D.; Xu, H.; Ye, L.; Hanif, M.; Liu, S. Y.; Ma, D. G.; Ma, Y. G. *J. Am. Chem. Soc.* **2005**, *127*, 14152. (b) Zhang, L.; Cao, Y.; Colella, N. S.; Liang, Y.; Bredas, J. L.; Houk, K. N.; Briseno, A. L. *Acc. Chem. Res.* **2015**, *48*, 500. (c) Xia, D.; Marszalek, T.; Li, M.; Guo, X.; Baumgarten, M.; Pisula, W.; Müllen, K. *Org. Lett.* **2015**, *17*, 3074. (d) Shi, L.; Liu, Z.; Dong, G.; Duan, L.; Qiu, Y.; Jia, J.; Guo, W.; Zhao, D.; Cui, D.; Tao, X. *Chem. - Eur. J.* **2012**, *18*, 8092. (e) Sahasithiwat, S.; Mophuang, T.; Menbangpung, L.; Kamtonwong, S.; Sooksimuang, T. *Synth. Met.* **2010**, *160*, 1148. (f) Pho, T. V.; Yuen, J. D.; Kurzman, J. A.; Smith, B. G.; Miao, M.; Walker, W. T.; Seshadri, R.; Wudl, J. *Am. Chem. Soc.* **2012**, *134*, 18185. (g) Okamoto, T.; Mitsui, C.; Yamagishi, M.; Nakahara, K.; Soeda, J.; Hirose, Y.; Miwa, K.; Sato, H.; Yamano, A.; Matsushita, T.; Uemura, T.; Takeya, J. *Adv. Mater.* **2013**, *25*, 6392.
- (6) (a) Lehnerr, D.; Hallani, R.; McDonald, R.; Anthony, J. E.; Tykewinski, R. R. *Org. Lett.* **2012**, *14*, 62. (b) Yanai, N.; Mori, T.; Shinamura, S.; Osaka, I.; Takimiya, K. *Org. Lett.* **2014**, *16*, 240. (c) Nakano, M.; Niimi, K.; Miyazaki, E.; Osaka, I.; Takimiya, K. *J. Org. Chem.* **2012**, *77*, 8099.
- (7) Liu, Y.; Shan, T.; Yao, L.; Bai, Q.; Guo, Y.; Li, J.; Han, X.; Li, W.; Wang, Z.; Yang, B.; Lu, P.; Ma, Y. *Org. Lett.* **2015**, *17*, 6138.
- (8) (a) Bonifacio, M. C.; Robertson, C. R.; Jung, J.-Y.; King, B. T. *J. Org. Chem.* **2005**, *70*, 8522. (b) Kar, G. K.; Haldar, M. K.; Gupta, S.; Pan, D.; Ray, J. K. *J. Indian. Chem. Soc.* **1999**, *76*, 569.
- (9) (a) Bosdet, M. J. D.; Jaska, C. A.; Piers, W. E.; Sorensen, T. S.; Parvez, M. *Org. Lett.* **2007**, *9*, 1395. (b) Jaska, C. A.; Emslie, D. J. H.; Bosdet, M. J. D.; Piers, W. E.; Sorensen, T. S.; Parvez, M. *J. Am. Chem. Soc.* **2006**, *128*, 10885.
- (10) Cinar, M. E.; Ozturk, T. *Chem. Rev.* **2015**, *115*, 3036.
- (11) Zhu, M. R.; Yang, C. L. *Chem. Soc. Rev.* **2013**, *42*, 4963.